Journal of Sound and Vibration (1998) **211**(3), 435–448

MULTI-PASS PERFORATED TUBE SILENCERS: A COMPUTATIONAL APPROACH†

N. S. DICKEY

Department of Mechanical Engineering and Applied Mechanics, The University of Michigan, Ann Arbor, Michigan 48109, *U.S.A.*

A. SELAMET

Department of Mechanical Engineering, The Ohio State University, 206 *West* 18*th Avenue, Columbus, Ohio* 43210-1107, *U.S.A.*

AND

J. M. NOVAK

Engine Product and Manufacturing Engineering, Ford Motor Company, Dearborn, Michigan 48121, *U.S.A.*

(*Received* 13 *April* 1996, *and in final form* 4 *March* 1997)

A time domain computational approach is applied to predict the acoustic performance of multiple pass silencers with perforated tube sections. This non-linear, one-dimensional method may readily include temporal and spatial variations in sound pressure level, orifice flow velocities, and mean duct flow, all of which affect the local orifice behaviour of perforated tube elements, and therefore the overall noise reduction characteristics. The transmission loss of two anechoically terminated multiple pass muffler configurations is determined computationally and experimentally for the limiting case of low sound pressure levels and zero mean flow. Comparisons between the numerical results and experimental data are shown to correlate well for frequencies where the one-dimensional assumption is justified.

1. INTRODUCTION

The silencing components used to reduce the sound radiated from automotive intake and exhaust systems often employ one or more perforated tube segments. For some elements, the overall structure may be complex enough to require a detailed, three-dimensional model to determine its general noise attenuation. However, for many practical configurations the relatively long wavelengths of the noise generated by the engine intake and exhaust processes allow simplified analyses. If the wavelength is much longer than any characteristic silencer dimension, a zero-dimensional, or lumped analysis, is valid and presents the least amount of difficulty. For an automotive silencer, zero-dimensional models may provide some insight at very low frequencies, but accuracy decreases rapidly with increasing frequency. Significant improvement from a lumped approach may be obtained by considering one-dimensional flow in the various silencer duct passages that communicate through the perforated interfaces. This coupled one-dimensional method is useful for low frequency acoustic analysis of many realistic silencer designs characterized

† An earlier and abbreviated version of this work was presented at the 1996 International Congress and Exposition of the Society of Automotive Engineers, February 26–29, 1996, Detroit, Michigan.

0022–460X/98/130435 + 14 $25.00/0/sv971318

by perforated tubes that are axially aligned within an external duct having a length that is substantially longer than any cross dimension. At higher frequencies, where the wavelength is not much longer than any cross dimension, or for very complex geometries, a coupled one-dimensional approach is no longer justified and multidimensional techniques need to be used.

The response of a perforated tube silencer is affected by the overall geometric structure, including duct porosities and orifice locations, and the perforate dynamics. The behavior of a perforated interface is usually presented in terms of a perforate impedance, $Z_{p,f}$, a frequency domain parameter given by

$$Z_{p,f} = \Delta p_{p,f} / U_{p,f}, \tag{1}$$

where Δp is the acoustic pressure difference, U is the area averaged velocity and the subscripts p and f refer to the perforate and fundamental frequency, respectively. It is well known that the dynamics of unsteady flow through an orifice are dependent on a number of local fluid-dynamic parameters in addition to the specific orifice geometry. Clearly the physical fluid properties (density, viscosity, etc.) are significant. Furthermore, the magnitude of the throughflow (mean plus oscillating), which is strongly coupled with the average pressure difference and sound pressure level across the perforate, causes drastic changes in the orifice behavior. Finally, the amount of grazing (axial duct) flow on either side of the perforate alters the local orifice dynamics.

For the conditions present in an automotive silencer, it is most likely that the perforated sections will exhibit non-linear behavior. For example, with zero mean flow, orifice non-linearity is observed at sound pressure levels on the order of 120–130 $dB_{re\ 20\ \mu Pa}$ [1], well below the levels accepted to be linear in one-dimensional duct acoustics and much lower than the magnitudes experienced in typical automotive intake and exhaust systems. Moreover, the values of fluid properties, acoustic pressure and bulk fluid flow can vary with both time and location. Since the perforate behavior depends on these parameters, it is reasonable to expect significant non-linearity at the perforate interfaces.

A number of studies have employed a coupled one-dimensional approach to study perforated tube geometries by using a linear wave equation to model the duct flows. The majority of these methods have been frequency domain approaches. Sullivan and Crocker [1] examined the acoustic performance of perforated concentric tube resonators under linear orifice conditions. Later Sullivan [2] analyzed one and two pass geometries using an iterative segmentation approach which has a much broader applicability, since it allows for spatial changes in the perforate impedance. However, the mean values of orifice and duct flow, need to be specified *a priori*. Analytical [3, 4] and numerical [5] decoupling techniques have also been applied to perforated tube geometries. In the analytical decoupling techniques, the perforate impedance and mean duct flow are assumed to be constant along a particular duct. The numerical decoupling approach of Peat [5] allows orifice impedances and mean flow to vary along a duct, although the mean flow must change linearly. Results for these decoupling analyses were presented for one and two pass silencers. Correlation between the foregoing frequency domain techniques and experimental data is generally quite good, provided that the geometry and flow conditions are consistent with the underlying assumptions of the particular method. As an alternative to frequency domain approaches, Chang and Cummings [6] have applied a numerical time-domain technique that uses a finite-difference approximation of the linearized one-dimensional wave equation in the main ducts, which may communicate *via* a non-linear orifice model. Since the solution proceeds in the time domain, temporal and spatial changes in orifice behavior may be accounted for. They obtained good correlation

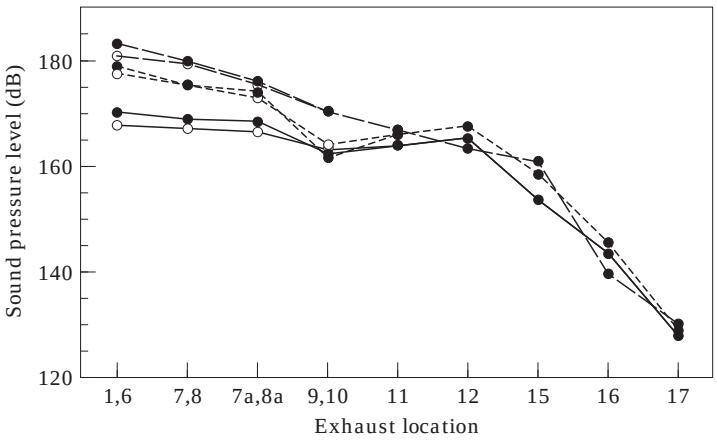

Figure 1. Measured sound pressure levels at different engine speeds for the exhaust system locations in Table 1: ——, 1000 r.p.m; -----, 3000 r.p.m.; — —, 5000 r.p.m.; ●, right bank; ○, left bank.

between computational and experimental results for high amplitude, non-harmonic wave propagation through a single pass resonator.

It is apparent that the analysis of a perforated tube silencer by itself can be a difficult task. For silencers placed in an internal combustion engine intake or exhaust system, this difficulty is compounded by a number of other factors. To determine accurately the sound radiated from any system, the source must be modelled accurately. For an automotive engine, this includes the highly non-linear processes taking place in the vicinity of the valves. In addition, flow losses created by the duct systems and silencers affect the backpressure (or inlet pressure) seen at the valve, and therefore modify the source characteristics. The experimental data shown in Figures 1 and 2 illustrate additional problems encountered when attempting to determine radiated sound levels of automotive engines. The variations in sound pressure level and mean temperature at wide open throttle conditions are shown for a Ford 1992 3.0L V-6 (Taurus) engine and production exhaust system. The data presented here are part of the experimental study by Selamet *et al*. [7]. In this system, the exhaust flows from the right and left banks are initially separate as the combustion products from three cylinders are combined in the manifold and sent through a short passage to a catalytic converter. Shortly after the catalytic converters, the

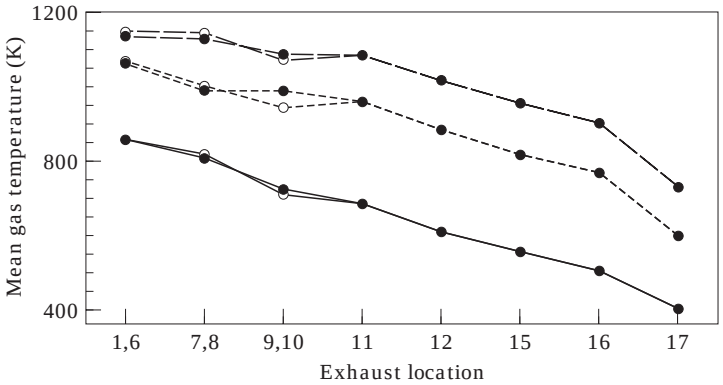

Figure 2. Measured mean temperatures at different engine speeds for the exhaust system locations in Table 1. Key as for Figure 1.

TABLE 1

Measurement location descriptions

Location	Description	Location	Description
1	Cylinder 1 primary runner	10	L.B. Catalytic converter exit
6	Cylinder 6 primary runner	11	Resonator inlet
7	R.B. manifold exit	12	Resonator exit
7a	R.B. catalytic converter inlet	15	Muffler inlet
8	L.B. manifold exit	16	Muffler exit
8a	L.B. catalytic converter inlet	17	Surge tank
9	R.B. catalytic converter exit		

right and left exhaust pipes merge into a single duct. After the exhaust flows merge, the fluid is passed through a small resonator, followed by another section of tubing and then the muffler. Beyond the muffler is a short tailpipe section connected to a large surge tank, implemented to dampen pressure oscillations in place of an expansion to ambient. Measurement locations are described in Table 1, where R.B. and L.B. denote the right and left engine banks, respectively.

The overall sound pressure levels for the locations described in Table 1 are depicted in Figure 1. These values are obtained from the measured time-domain data as

$$\mathrm{SPL(dB)} = 10 \log_{10}\left[\frac{1}{\Delta t}\int_{t}^{t+\Delta t}\left(\frac{p-\bar{p}}{p_{ref}}\right)^2 \mathrm{d}t\right], \tag{2}$$

where Δt is the time period for one complete engine cycle (two revolutions), $\bar{p}$ is the average pressure at the sampling point, and $p_{ref} = 20\ \mu\mathrm{Pa}$. At locations upstream of the catalytic converters, SPL values range from approximately 167 dB to well over 180 dB. Oscillations of this magnitude would indicate that non-linear effects may also be significant in the interactions between the main runners in addition to the processes occurring at the valve. Inlet sound pressure levels of approximately 164–166 dB and 154–161 dB for the resonator and muffler, respectively, show that the perforated components in these elements are almost certainly acting in a non-linear fashion, although grazing flow and perforate throughflow will affect their response and require additional consideration.

In the exhaust system, the speed of sound (or, equivalently, the wavelength of a given frequency) at a point will mainly depend on the local temperature. Figure 2 shows the variation in mean temperature with both distance from the exhaust port and engine speed. For the 1000 r.p.m. case, the mean temperature varies from approximately 825 to 500 K between locations 1 and 16. With respect to the primary runner, the relative change in the mean speed of sound between these locations is approximately

$$\Delta c_{16-1}/c_1 \simeq \sqrt{T_{16}/T_1} - 1 = -0{\cdot}22, \tag{3}$$

resulting in a 22% shift in the wavelength of a specific frequency component. The large differences seen in the temperature at a fixed location for different engine speeds also require consideration.

For approaches using linearized equations to analyze unsteady duct flows, the applicability to an overall intake or exhaust system becomes questionable. Moreover, these approaches require a fixed source boundary condition, such as an input waveform or source impedance to represent the engine (see, for example, Gupta and Munjal [8]). Therefore changes in the system design which affect the flow through the valves (by

changing backpressure or system dynamics) may only be included externally and require separate analytical techniques. The complexity and numerous non-linearities observed in automotive intake and exhaust systems suggests the need for a method that can accurately model these phenomena. Non-linear one-dimensional techniques have proven useful for predicting intake and exhaust system flows in the ducts of automotive engines [9–12]. These techniques have mainly been used to study the effects of intake and exhaust system geometry on engine performance parameters (volumetric efficiency, power, etc.), although some simple silencers have been considered. More recently, analysis of single pass perforated tube geometries for low sound pressure levels and zero mean flow has been performed [13, 14].

The objective of the current study is to apply a non-linear fluid dynamic model to predict the transmission loss of multiple pass perforated tube silencers a typical example of which is shown in Figure 3. The multiple pass geometries, selected to be more representative of realistic mufflers, are modelled under low sound pressure level and zero mean flow conditions. The numerical method employed is an extension of the non-linear, one-dimensional finite difference scheme used by Chapman *et al*. [11]. In an earlier work [14] this technique was applied to model single pass perforated tube silencers under zero mean flow and low sound pressure level conditions. Good agreement was obtained with experimental results for both short and long concentric tube resonators. Since the technique is applicable to practically any geometry, provided that one-dimensional flow is justified, it can be used to model the entire intake and exhaust system, accounting for variations in flow dynamics that are dependent on the engine, manifold and silencer configurations. In addition, the computational program connects the ducts, perforated tubes and volumes which comprise the silencer in a modular fashion, so that multiple pass element models are readily described in a program input file.

Though the numerical technique is applicable for the numerous non-linearities observed in automotive intake and exhaust systems, the present study is restricted to the low sound pressure level, zero mean flow regime. This limit is chosen to allow comparisons between the computational results and the experimental data for multiple pass perforated tube elements in an anechoically terminated impedance tube test facility.

2. DUCT NUMERICS

The governing balance equations of mass, momentum and internal energy for an unsteady, compressible flow may be expressed as

$$\partial\rho/\partial t + \mathbf{\nabla}\cdot(\rho\vec{U}) = 0, \tag{4}$$

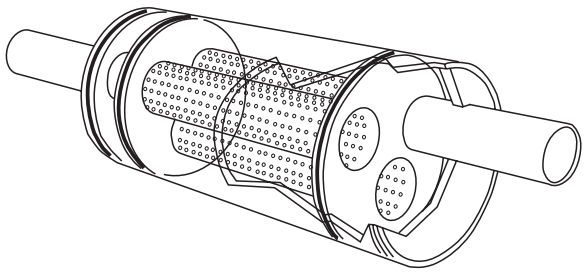

Figure 3. Geometry of the test muffler.

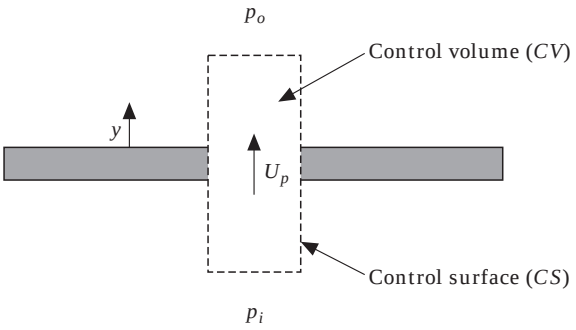

Figure 4. Nomenclature and control volume used for application of momentum equation to a single orifice.

$$(\partial/\partial t)(\rho\vec{U}) + \nabla\cdot(\rho\vec{U}\vec{U}) + \nabla p - \nabla\cdot\bar{\bar{\tau}} = 0, \tag{5}$$

$$(\partial/\partial t)(\rho e) + \nabla\cdot(\rho\vec{U}e) + p\nabla\cdot\vec{U} - \bar{\bar{\tau}}\colon\nabla\vec{U} + \nabla\cdot\vec{q} = 0, \tag{6}$$

where ρ is density, U is velocity, p is pressure, $\bar{\bar{\tau}}$ is the shear stress tensor, e is the specific internal energy and q is the heat flux. The ideal gas equation of state,

$$p = (\gamma - 1)\rho e, \tag{7}$$

where γ is the ratio of specific heats, is used to relate the thermodynamic variables and close the system of equations. Equations (4)–(7) are discretized for one-dimensional flow in ducts of variable cross-section by employing the explicit finite difference method of Chapman *et al*. [11] as discussed by Selamet *et al*. [15]. Since the numerical treatment of the duct flows is essentially unchanged by the incorporation of perforate communication, the following description will focus only on the orifice flow treatment in the model. Details of the one-dimensional duct numerics may be found in references [11] and [15].

For the perforate interface model, it is assumed that the locally incompressible orifice flows act independently. Application of the y-direction momentum equation to a single orifice, as shown in Figure 4 yields, in integral form,

$$\frac{\mathrm{d}}{\mathrm{d}t}\int_{CV}\rho U_y\,\mathrm{d}V = (p_i - p_0)A_p - \int_{CS}\tau_y\,\mathrm{d}A - \int_{CS}\rho U_y(\vec{U}\cdot\hat{\mathbf{n}})\,\mathrm{d}A, \tag{8}$$

where the subscripts CV and CS denote the control volume and control surface, respectively, A_p is the orifice area and $\hat{n}$ is the unit outward normal vector. For low sound pressure levels and zero mean flow, the convective term on the right side of equation (8) may be neglected, resulting in a balance between the inertial, pressure and viscous forces as

$$\frac{\mathrm{d}}{\mathrm{d}t}\int_{CV}\rho U_y\,\mathrm{d}V = (p_i - p_0)A_p - \int_{CS}\tau_y\,\mathrm{d}A. \tag{9}$$

Equation (9) is further simplified to

$$M_{eq}\,\mathrm{d}U_p/\mathrm{d}t = (p_i - p_0)A_p - RU_pA_p, \tag{10}$$

where the coefficients M_{eq} and R represent an equivalent mass and equivalent resistance, respectively. Division by A_p yields the expression employed in the current model as

$$\rho l_{eq}\, \mathrm{d}U_p/\mathrm{d}t = p_i - p_0 - RU_p, \tag{11}$$

where $l_{eq} = M_{eq}/A_p$ is an equivalent length for the orifice. This treatment is equivalent to the work of Sullivan and Crocker [1], although the solution proceeds in the time domain rather than being determined in the frequency domain. In contrast to the frequency domain approaches, the values for the effective length l_{eq} and flow resistance R may be determined from the instantaneous local fluid dynamics, and therefore may vary with position and time.

Due to the complexity of the unsteady flow through an orifice, analytical approximations for l_{eq} and R only exist for the simplest of conditions. Consequently, empirical data is generally required. Although a number of experimental studies have been performed to analyze the effects of high sound pressure levels, mean throughflow and grazing flow [16–20], the findings are almost exclusively presented in terms of a non-linear orifice impedance referenced to a single excitement frequency. Therefore these results may only be used approximately to determine the variable coefficients R and l_{eq} for arbitrary input waveforms. Cummings [16] has presented an essentially equivalent orifice flow model incorporating variable coefficients for the case of zero mean flow and no grazing flow. In addition, Chang and Cummings [6] employed frequency domain experimental data in a time domain approach to model a single pass concentric tube resonator under multiple frequency excitation. For the limiting case considered here, l_{eq} and R are assumed constant and are taken from reference [1].

The numerical model employs a staggered mesh that divides a duct into cells with vector quantities located at node points and scalar quantities at cell midpoints. For a given computational cell containing perforations, the orifice area and perforate flow are assumed to be evenly distributed over the wall area. Figure 5 depicts the reduction of a single pass perforated tube silencer into inner and outer control volumes and shows the variable centering used. In the numerical model, equation (11) is approximated as

$$\rho^n l_{eq}(U_p^{n+1} - U_p^n)/\Delta t = p_i^n - p_0^n - RU_p^n, \tag{12}$$

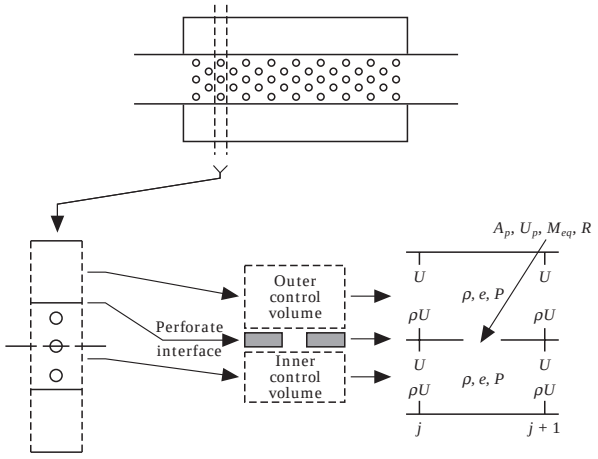

Figure 5. Physical element reduction and variable centering for the numerical technique.

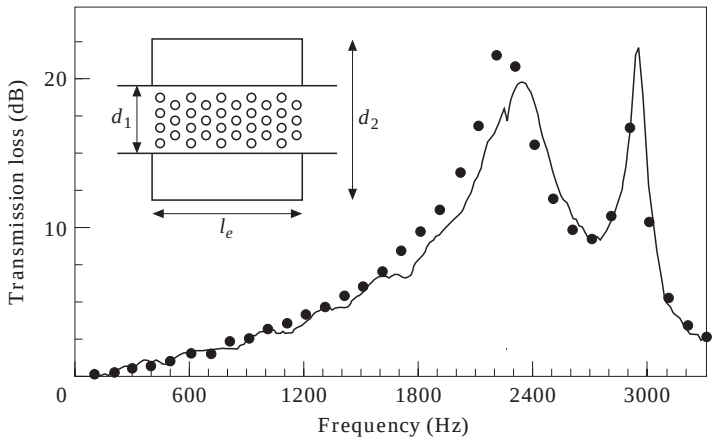

Figure 6. Transmission loss for a "short" concentric resonator ($d_1 = 5{\cdot}08$ cm; $d_2 = 7{\cdot}62$ cm; $l_e = 6{\cdot}67$ cm; $\sigma = 0{\cdot}037$): ——, experiment; ●, model.

where the superscript n denotes the timestep. Once the updated perforated velocity is calculated from equation (12), the mass and internal energy fluxes through the orifice are computed using upwind differencing.

3. RESULTS

The computational model has been applied to a number of perforated tube silencers, consisting of both single and multiple pass geometries. One particular configuration, the single pass concentric tube resonator, has received much attention due to its practical significance and relatively simple geometry [1–4, 6, 13, 14, 21]. For comparative purposes, the experimental and computational results for two such configurations are included here. The geometries considered are evenly perforated over the central tube (see inset Figure 6), and have dimensions consistent with the "short" and "long" resonators considered in more detail by Sullivan and Crocker [1], as shown in Table 2. Figures 6 and 7 compare the results of the numerical model with experimental data for the short and long resonators, respectively. For both geometries, the predictions from the numerical model are in close agreement with experimental data.

The geometry of the first multi-pass test muffler, a three pass configuration, is shown in Figure 3. In this silencer, the fluid travels along the entrance duct to the first end chamber, reverses direction and travels to the second end chamber through the pass tube, and reverses direction once more prior to leaving the muffler in the exit tube. Travelling oscillations in all three ducts communicate with the outer cavity over the central section of the muffler. The three interior ducts have an outer diameter of 5·08 cm and a 0·08 cm wall thickness, while the external casing is fabricated from a 16·51 cm inner diameter

TABLE 2

Geometry of short and long resonators

Resonator	l_e (cm)	d_1 (cm)	d_2 (cm)	t_{wall} (cm)	Porosity (σ)	$d_{orifice}$ (cm)
Short	6·67	5·08	7·62	0·079	0·037	0·249
Long	25·72	5·08	10·15	0·079	0·020	0·249

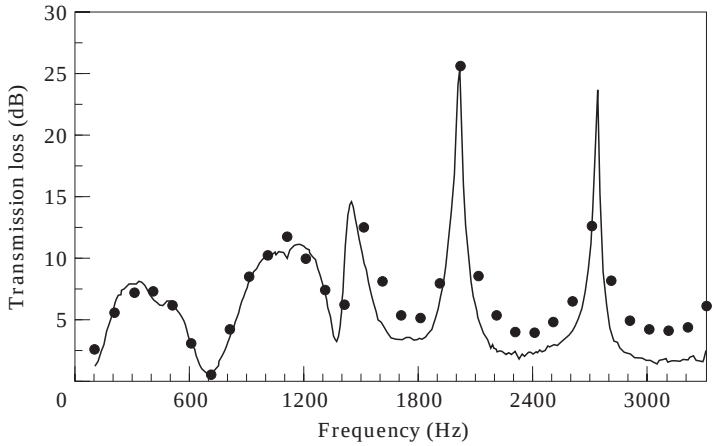

Figure 7. Transmission loss for a "long" concentric resonator ($d_1 = 5{\cdot}08$ cm; $d_2 = 10{\cdot}15$ cm; $l_e = 25{\cdot}72$ cm; $\sigma = 0{\cdot}020$): ——, experiment; ●, model.

polycarbonate tube. The end chambers are separated from the 25·5 cm long central cavity by 1·27 cm thick baffles, and have volumes of 831 cm^3 and 892 cm^3. Interior duct porosities of 4·8% were created by drilling 400 holes of 0·249 cm diameter in each duct over the central region. To account for the local multidimensional effects at the expansion from the central tubes to the end chambers, a small end correction is necessary. For simplicity, the end correction is determined from the work of Ingard [22] for concentric Helmholtz resonators as

$$\delta = 0{\cdot}425 d_p \left(1 - 1{\cdot}25 \frac{d_p}{d_V}\right), \tag{13}$$

where d_p and d_V are the pipe and cavity diameters, respectively.

Computational results for the three pass silencer are compared to experimental data in Figure 8. Correlation between the model and experiment is satisfactory up to approximately 1000 Hz, where multidimensional effects become significant. Note that this frequency is slightly lower than the limit for continuous propagation of the first diametral mode in a circular duct, given by $f_{\text{first diametral mode}} = 1{\cdot}84 c_0/\pi d_{\max} = 1220$ Hz, for a speed of sound of 344 m/s in air at atmospheric conditions. Some discrepancy between the model and experiment is also seen at frequencies below 150 Hz, which may be attributed to slight imperfections in the experimental facility anechoic termination. The overall behavior is similar to an expansion chamber with a superimposed resonance near 450 Hz. Since the central section is effectively an expansion chamber, it appears that the end chambers are behaving as Helmholtz resonators (the end chamber volumes are very similar, so both should resonate at approximately the same frequency). Assuming the two pipes attached to an end chamber act synchronously, and using an average of the two end volumes, the effective neck length necessary for a resonance frequency of 450 Hz is approximately 6·4 cm. If the perforations are assumed to be transparent, and equation (13) is applied at both ends of the baffle, the effective neck length is

$$l_0 + 2\delta = 4{\cdot}44 \text{ cm}, \tag{14}$$

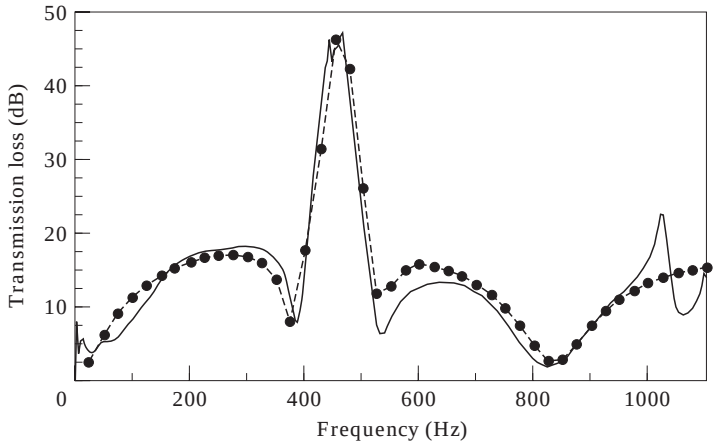

Figure 8. Transmission loss of three pass muffler: ——, experiment; --●--, model.

where l_0 is the axial distance between the volume side of the baffle and the first row of orifices. Therefore, the perforated sections do not repress the interaction between the end volumes and central chamber substantially, but show their presence by augmenting the effective neck length.

The sensitivity of perforated tube silencers to variations in porosity is demonstrated in Figure 9, which shows the computed transmission loss of the three pass muffler for three different duct porosities. The highest porosity shown (5%) is very close to the value for the fabricated geometry, and therefore has essentially the same behavior seen in Figure 8. As the porosity is reduced, the inhibited communication between the end chambers and the central cavity becomes more noticeable. This effect causes a reduction of the resonance frequency (or, equivalently, an increase in the effective neck length) accompanied by a decrease in the transmission loss magnitude near the resonance frequency. As expected, the deviations from the expansion chamber behavior increase as the porosity is reduced. The departure from an overall dome-like behavior is most prevalent for the 1% porosity

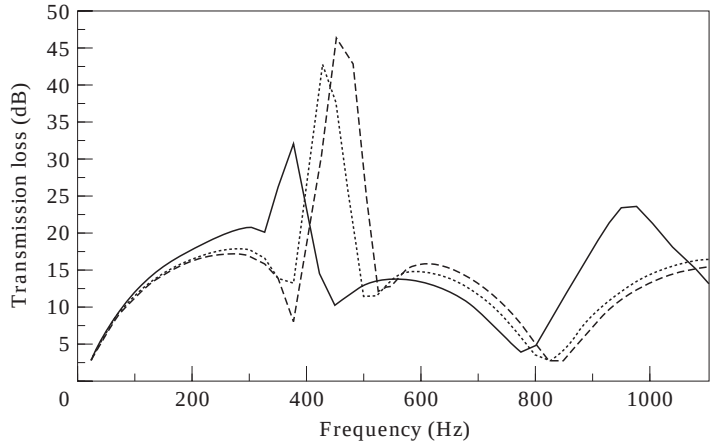

Figure 9. Predicted transmission loss of three pass muffler for different porosities: ——, $\sigma = 0{\cdot}01$; · · · ·, $\sigma = 0{\cdot}03$; – – –, $\sigma = 0{\cdot}05$.

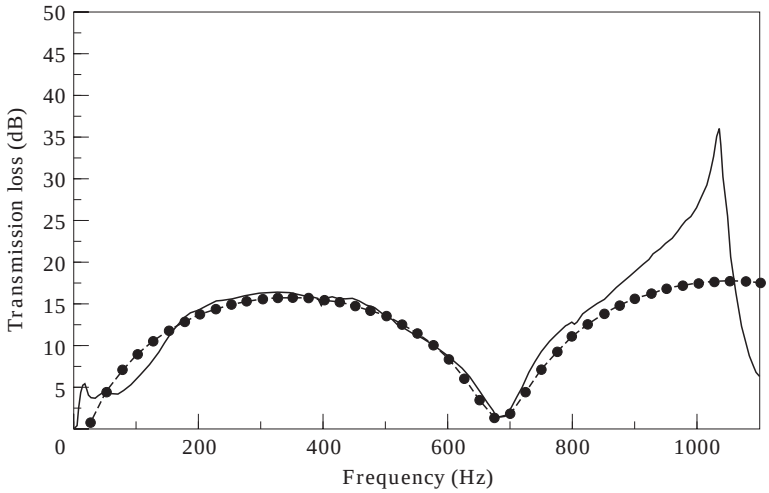

Figure 10. Transmission loss of two pass cross-flow muffler: ——, experiment; --●-, model.

case, which shows a noticeable shift of the transmission loss minimum near 825 Hz, followed by a secondary peak much sharper and of greater magnitude than the higher porosity cases.

The second multi-pass geometry considered in the study is a two pass cross flow element. To create this configuration, the three pass muffler was modified by removing the pass tube, sealing the holes in the baffles where the pass tube was removed, and sealing the ends of the inlet and exit ducts. These changes allow the inlet and exit ducts to communicate over the central cavity, and remove the end chambers entirely. Though this created a simpler silencer, asymmetry of the structure actually increased somewhat, so multidimensional effects should be expected to occur at or slightly below the limiting frequency of the first muffler. Figure 10 compares the model predictions with experimental results for this configuration. Multidimensional effects are seen to become significant near 900 Hz, below which the behaviour shows the repeating broadband domes of a simple expansion chamber. Assuming the perforated tubes to be transparent, the chamber has an expansion ratio of $m = 11{\cdot}27$ and length $l_e = 25{\cdot}5$ cm. Therefore the domes should have a maximum value of $10 \log_{10}(1 + 0{\cdot}25(m - 1/m)^2) = 15{\cdot}1$ dB, and repeat at intervals of $\Delta f = c_0/2l_e = 674$ Hz, which are very close to the data for the first dome in Figure 10. Since the model assumes one-dimensional fluid motion, it continues to predict an expansion chamber behavior beyond 900 Hz, as expected.

4. CONCLUDING REMARKS

A one-dimensional, finite difference numerical solution of the fundamental balance equations for unsteady, compressible flow has been shown to accurately predict the attenuation of sound in multiple pass perforated tube silencer elements. This method avoids many of the restrictions that are inherent in frequency domain techniques. Although the present study considers acoustic disturbances in a quiescent medium only, the method is capable of treating high sound pressures and complex flow fields, including shock waves, provided that the one-dimensional assumption is justified and a suitable model for perforate flow is incorporated. Although diametral modes will not continuously propagate along a duct at frequencies below $\pi d/\lambda = 1{\cdot}841$, and this expression is commonly used to determine the upper frequency limit of one-dimensional approaches, it has been shown that

multidimensional behavior may become significant at slightly lower frequencies for fairly complex perforated tube systems. Since the geometries considered are more representative of exhaust system silencers, a 900 Hz upper frequency limit determined at atmospheric conditions is rather conservative. For example, scaling the upper limit with respect to a speed of sound of approximately 450 m/s in the exhaust gas (based on a gas temperature of 500 K, roughly corresponding to the muffler conditions at 1000 r.p.m. in Figure 2), shows that the one-dimensional assumption is valid for modelling the above mufflers to frequencies of about 1180 Hz. This limit is high enough to include the firing fundamental and first few harmonics of most engines even at relatively high speeds (for example, a six-cylinder engine running at 5000 r.p.m. has a firing fundamental of 250 Hz). A number of studies are available on the analysis of flow through orifices under various conditions, including high sound pressure levels, through-flow and grazing flow [18, 23]. Work is currently in progress to incorporate these factors in the present perforate model. The non-linear, time-domain approach is expected to be useful for a wide range of applications, including complex geometries, non-linear flow phenomena and entire engine intake and exhaust systems.

REFERENCES

1. J. W. Sullivan and M. J. Crocker 1978 *Journal of the Acoustical Society of America* **64**, 207–215. Analysis of concentric-tube resonators having unpartitioned cavities.
2. J. W. Sullivan 1979 *Journal of the Acoustical Society of America* **66**, 772–788. A method for modeling perforated tube muffler components. I. Theory. II. Applications.
3. K. Jayaraman and K. Yam 1981 *Journal of the Acoustical Society of America* **69**, 390–396. Decoupling approach to modeling perforated tube muffler components.
4. M. L. Munjal, K. N. Rao and A. D. Sahasrabudhe 1987 *Journal of Sound and Vibration* **114**, 173–188. Aeroacoustic analysis of perforated muffler components.
5. K. S. Peat 1988 *Journal of Sound and Vibration* **127**, 123–132. The acoustical impedance at discontinuities of ducts in the presence of a mean flow.
6. I. J. Chang and A. Cummings 1988 *Journal of Sound and Vibration* **122**, 243–259. A time domain solution for the attenuation, at high amplitudes, of perforated tube silencers and comparison with experiment.
7. A. Selamet, S. H. Yonak, J. M. Novak and M. Khan 1995 *SAE* 951260. The effect of vehicle exhaust system components on flow losses and noise in firing spark-ignition engines.
8. V. H. Gupta and M. L. Munjal 1992 *Journal of the Acoustical Society of America* **92**, 2716–2725. On numerical prediction of the acoustic source characteristics of an engine exhaust system.
9. G. P. Blair and S. W. Coates 1973 *SAE* 730160. Noise produced by the unsteady exhaust efflux from an internal combustion engine.
10. G. P. Blair and J. H. McConnell 1974 *SAE* 740736. Unsteady gas flow through high-specific-output 4-stroke cycle engines.
11. M. Chapman, J. M. Novak and R. A. Stein 1982 In *Flows in Internal Combustion Engines*. (editor, Teoman Uzkan). Numerical modeling of inlet and exhaust flows in multi-cylinder internal combustion engines. ASME WAM, Austin, TX.
12. T. Morel, M. F. Flemming and L. A. LaPointe 1990 *SAE* 900679. Characterization of manifold dynamics in the Chrysler 2.2 s.i. engine by measurements and simulation.
13. T. Morel, J. Morel and D. A. Blaser 1991 *SAE* 910072. Fluid-dynamic and acoustic modelling of concetric-tube resonators/silencers.
14. A. Selamet, N. S. Dickey and J. M. Novak 1993 In *Proceedings of NOISE-CON* 93 (editor, H. H. Hubbard) pp 291–296. A time domain based computational approach for perforated tube silencers.
15. A. Selamet, N. S. Dickey and J. M. Novak 1994 *Journal of the Acoustical Society of America* **96**, 3177–3185. The Herschel–Quincke tube: A theoretical, computational, and experimental investigation.
16. A. Cummings 1986 *Journal of the Acoustical Society of America* **79**, 942–951. Transient and multiple frequency sound transmission through perforated plates at high amplitude.

17. A. L. Goldman and R. L. Panton 1976 *Journal of the Acoustical Society of America* **60**, 1397–1404. Measurement of the acoustic impedance of an orifice under a turbulent boundary layer.
18. T. H. Melling 1973 *Journal of Sound and Vibration* **29**, 1–65. The acoustic impedance of perforates at medium and high sound pressure levels.
19. U. Ingard and H. Ising 1967 *Journal of the Acoustical Society of America* **42**, 6–17. Acoustic nonlinearity of an orifice.
20. E. Feder and L. W. Dean III 1969. *NASA CR*-1373. Analytical and experimental studies for predicting noise attenuation in acoustically treated ducts for turbofan engines.
21. K. S. Peat 1988 *Journal of Sound and Vibration* **123**, 199–212. A numerical decoupling analysis of perforated pipe silencer elements.
22. U. Ingard 1953 *Journal of the Acoustical Society of America* **25**, 1037–1061. On the theory and design of acoustic resonators.
23. D. Ronneberger 1972 *Journal of Sound and Vibration* **24**, 133–150. The acoustical impedance of holes in the wall of flow ducts.

NOMENCLATURE

A	area
c	speed of sound
CS	control surface
CV	control volume
d	diameter
e	specific internal energy
f	frequency
k	$= 2\pi f/c_0$, wavenumber
l	length
m	expansion ratio
M	mass
p	pressure
q	heat transfer rate
R	perforate flow resistance
t	time
T	temperature
U	velocity
V	volume
x	rectangular co-ordinate
y	rectangular co-ordinate
Z	impedance

Greek Symbols

γ	ratio of specific heats
δ	end correction
Δ	difference
λ	wavelength
ρ	density
σ	porosity
$\bar{\bar{\tau}}$	shear stress tensor

Subscripts

e	expansion chamber
eq	equivalent
i	inner
f	frequency
max	maximum

o	outer
0	mean value
p	perforate
ref	reference
V	volume
y	y-direction

Superscripts

n	timestep